

# THE INFLUENCE OF HALL CURRENT AND THERMAL RADIATION ON THE BLOOD FLOW OF WILLIAMSON NANOFLUID IN AN INCLINED DISEASED ARTERY PRESENCE OF HEAT AND MASS TRANSFER

G. SHANKAR, E.P. SIVA \*

Department of Mathematics, College of Engineering and Technology, SRM Institute of Science and Technology,  
Kattankulathur, Chengalpattu, Tamilnadu - 603203, India

\*Corresponding author: sivae@srmist.edu.in

Received Oct. 3, 2023

**ABSTRACT.** The prevalence of cardiovascular illnesses remains a prominent issue in global health, underscoring the need for a deeper understanding of the hemodynamic characteristics of the arteries affected by these disorders. The objective of this research is to examine the complex relationship between hall current, heat radiation, and the flow properties of Williamson nanofluid in an inclined diseased artery. The consideration of heat and mass transport effects is also undertaken to understand their influence on the physiological environment. A mathematical framework is constructed by integrating the Navier-Stokes equations with energy and concentration equations to characterise the flow dynamics. The main (governing) dimensional equations of the Williamson nanofluids under consideration are initially transformed into dimensionless ordinary differential equations (ODEs) using appropriate analogous variables. The system of equations is calculated using the `bvp4c` technique. The incorporation of the hall current, which quantifies electromagnetic force, and thermal radiation, which arises from temperature disparities, is included in the model to explicate their impacts on blood circulation. The findings suggest that the inclusion of hall current and thermal radiation has a substantial impact on the velocity and temperature distributions inside the affected artery. Additionally, the incorporation of Williamson nanofluid particles displays discernible attributes in augmenting or reducing rates of heat and mass transfer, thus influencing the overall dynamics of the flow. The present study provides significant contributions to the understanding of intricate fluid dynamics and heat/mass transfer mechanisms occurring in sick arteries. These findings offer useful insights that might potentially enhance treatment efficacy and patient care in the field of cardiovascular medicine.

2020 Mathematics Subject Classification. 76Z05.

Key words and phrases. blood flow; hall current; stenosis inclined artery; thermal radiation; Williamson nanofluid.

## 1. BACKGROUND AND INTRODUCTION

The primary role of the cardiovascular system is to deliver the nutrients and oxygen needed for the functioning of the body's tissues. Additional goals include getting rid of waste, maintaining the temperature, and transporting vital substances like hormones or antibodies throughout the cell. The medical term "stenosis" refers to the constriction of an artery due to the growth of abnormal tissue or the accumulation of atherosclerotic plaque. This development, as it advances into the lumen of the artery, restricts blood flow. This blockage has the ability to harm the inner wall cells, making the stenotic condition even worse. A major disturbance called stenosis can occur in blood vessels, which will result in poor blood circulation in our body. Therefore, there is a reciprocal relationship between the development of stenosis and blood flow within the artery. When the blood flows quickly, a high amount of stress is placed close to the blood vessel's stenosed point, and this tension may cause major bodily harm. Also, it is evident that the non-dimensional maximal velocity is exponentially increased when it is shown for all stenosis nodes at a particular degree of constriction (stenosis). Individually strong stenotic flow characteristics can be predicted using various simulation techniques. It may also be applied to researching additional parametric influences Jung et al. [1]. Using simulations, the impact of stenosis on the pulsatile blood circulation in curved arteries with stenosis at the inner surface of the wall was examined by Liu [2]. They reported that the characteristic variation in the flow that was noticed downstream may indicate the creation of a new plaque. Qiao et al. [3] investigated different aspects of geometry, like S-shaped blood vessels in pulsatile flow through curved arteries. The influences of flexible (elastic) and viscoelastic walls are compared in pulsatile blood flow through a stenosed artery, as explained by Nejad et al. [4]. Goswami et al. [5] considered a power-law fluid model in rigid stenosed arteries along with slip conditions and magnetic fields. Kalita and Schaefer [6] explained the mechanical characteristics of the elastic wall of the artery. Furthermore, we dealt with three-dimensional nonlinear equations solved by numerical technique. When shear stress is lower than yield stress, the Bingham model predicts that the shear rate will quickly collapse to zero. So, shear stress is not dependent on shear rate. It is very difficult to solve the constitutive equation, but it is solved easily by applying bi-viscosity. Ishikawa et al. [7], [8] explained two distinct types of non-Newtonian fluid, which are tangent hyperbolic fluid and Bingham plastic fluid in blood flow inside the stenosed tube. The movement of blood through the arteries can be controlled with the aid of magnets discovered by Debberma and Srivastava [9]. Lee et al. [10] examined wall characteristics and flow modelling using a 3D ultrasound image. In addition to that model, they figured out the geometry to be a 45 % stenosed-affected region in the blood flow. They also reveal that the numerical result will be helpful for improving the effectiveness of pharmaceutical therapy and bypass design for specific people. Long et al. [11] investigated a comparison between the three different severe positions of constrictions (25 %, 50 % and 75 %) in pulsatile blood flow in the stenosis artery. Moreover, flow

features [velocity profile, flow separation zone, and wall shear stress] were evaluated. Sriyab [12] discovered the interaction between the peculiar form and size of restricted arteries, known as stenotic geometry, and the distinct features of blood flow, characterised by non-Newtonian behavior. Sweed et al. [13] investigated two-phase (fluid and particle) blood flow in asymmetric stenosis arteries with heat and mass transfer and made a comparison between steady and unsteady state situations. Zaman et al. [14] studied the cross non-Newtonian blood flow model in tapered stenosed arteries and applied viscous dissipation. This study suggested that both arterial curvature and plaque (lipid) deposition play a major role in drug distribution and the treatment of diseases.

In the field of medicine, magnetohydrodynamics (MHD) has an essential function, especially in the treatment of hyperthermia and malignant tumours, and controls the flow of magnetic wound haemorrhage during surgery. Many of the desirable functions are available due to the enormous applications of magnetohydrodynamics in bioscience, medical engineering, and bionic structures in the present year. Das et al. [15] examined the impact of the electromagnetic field on a hybrid nanofluid when administered through an endoscope. The investigation considered the influence of ion slip and hall currents, as well as the presence of peristaltic waves. It has been shown that altering the characteristics of waveforms has a strong effect on the generation of the streamlined pattern that represents the characteristics of blood circulation. An electric field is formed perpendicular to both the flow of charge carriers and the magnetic field when a current-carrying conductor is placed in a magnetic field that is perpendicular to the flow of current. This field is known as the Hall field, and the associated effect is known as the Hall effect. The application of the Hall effect is to find the type of semiconductor and carrier concentration and calculate the mobility of the charger carrier. Mekheimer and El Kot [16] investigated the effects of hall current and magnetic field on the micropolar blood flow model in stenosed arteries. These effects will clarify magnetic resonance angiography (MRA). Akbar and Butt [17] explained the effects of Cu nanoparticle blood flow in the presence of a magnetic field inside the composite stenosed arteries. They introduced copper-water-based nanoparticles and applied lubrication techniques to solve the governing equations. El Kot and Elmaboud [18] discussed LDL-C (Lipid Low-Density Lipoprotein Concentration) of the blood flow model in multiple stenosis arteries. Afzal et al. [19] explained three types of important radioactive materials in blood flow under MHD and slip conditions. They reveal that a rise in the volume percentage of radioactive elements causes blood flow through walls to increase in both the radial and tangential axes. Ohm's law is used in the account of grasping the impacts of the Hall current (effect) and magnetic field by Bhatti and Rashidi et al. [20] and figured out the sway of Eckert number ( $Ec$ ) and Prandtl number ( $Pr$ ) have increased temperature profile. The concepts of peristaltic motion theory, linear approximation heat flux, and heat radiation are all combined and applied to flow problems. This phenomenon is feasible only in the situation of variable differences in temperature considered from fluid flow. Asha and Sunitha [21] investigated

the significance of double diffusion, hall effects, and heat (thermal) radiation on the phenomenon of peristaltic nanoparticle blood flow. Kothandapani and Prakash [22] examine how a magnetic field and thermal radiation affect the peristaltic motion of Williamson nanofluids. Sharma et al. [23]- [26] investigated fluid models, changing viscosity in a two-phase fluid (Plasma and Core) and the Casson blood fluid through a curved stenosis artery under the influence of magnetohydrodynamics (MHD). Here, the plasma region has variable viscosity, and the core region has constant viscosity. Tripathi and Sharma extended the presence of inclined channels along with the parameters of chemical reactions and radiation. Their findings demonstrate that the amount of wall shear stress at the stenosis neck in an inclined artery increases with increasing values of the applied magnetic field while decreasing with an increase in the values of the chemical reaction and permeability parameters. Here, single and two-phase models are compared to experimental results. It shows that two-phase fluid has better results compared to single-phase fluid. In recent days, more attention has been given to nanofluid and hybrid nanofluid. It is very helpful for many fields like medicine, engineering, and industries. Another study in question is to analyse the effects of permeability on blood circulation by considering hybrid nanoparticles passing via a bifurcated stenosed artery by Shahzadi and Bilal [27] and reveals that when an atherosclerotic artery experiences bifurcation factors, permeable effects are much more efficient. In order to achieve the necessary heat flow rate during surgical procedures, trihybrid nanofluids of dissimilar shapes are used. At increased loadings of trihybrid nanoparticles injected into the bloodstream, a decreased temperature profile is observed by Karmakar et al. [28]. Zaman et al. [29] applied aluminium dioxide and silver (hybrid) nanoparticles to investigate the flow motion of blood in both stenosis and aneurysm arteries with time-dependent behavior. Das et al. [30] investigated the significance of Hall currents in the context of hybrid nano-blood flow in an inclined artery with modest stenosis. The homotopy perturbation approach is utilised in order to examine the influence of these currents on the circulation of blood under such circumstances. Mehmood et al. [31] investigated especially applying boundary conditions in both segments of stenosis and aneurysm inside a balloon catheter artery. Ali et al. [32] considered the influence of an electric double layer of Jeffery hybrid nanoparticles through the peristaltic microtube. Elnaqeeb [33] applied a radial-direction magnetic field to the Cather multiple stenosis artery using gold nanoparticles. They reveal that the arterial wall may be harmed by changing the value of the magnetic field. Alanazi et al. [34] explained that the thermal (heat) transfer rates measured by thermophoresis and Brownian motion flow result in steadily increasing behaviour on the channel's upper wall and decreasing behaviour on its lower wall. The crucial point is that hybrid nanoparticles were more effective than only the use of nanoparticles for enhancing thermal conductivity, heat transfer rate, and the nano-layer. Tripathi et al. [35], [36] studied a comparison between nano and hybrid (silver, gold) nanoparticles in overlapping stenosis arteries in the presence of MHD. Here is the clinical data for hemodynamic results. Tripathy et al. investigated a phase blood flow model with k-th order chemical

reactions. Additionally, we examined the parameters of joule heating and viscous dissipation. Zain and Ismail [37] considered the model of generalised power law in the presence of MHD on blood flow through overlapping bifurcated stenosis arteries and solved it by numerical technique. Ahmed and Nadeem [38] investigated the effects of the different shapes of copper nanofluid on time-dependent blood flow through a curved catheterized stenosis artery. Poonam et al. [39] investigated the hematocrit-dependent viscosity of hybrid nanoparticle flow in the stenosis artery. They concluded that applying external radiation to cancer treatment will reduce the creation and growth of arteriosclerosis. Nadeem et al. [40], [41] investigated the impact of heat, chemical reactions, and material transfer on blood flow in arteries characterised by narrowing (tapering) and obstructions (stenosis). The study specifically centres around utilising a distinct biomagnetic and Williamson fluid.

Using the literature review as an overview, the objective of this study is to examine the influence of thermal radiation and hall currents on the flow characteristics of a Williamson nanofluid within an inclined artery that displays mild stenosis. This investigation enhances our understanding of magnetic resonance angiography, a vital radiological diagnostic technique utilised in the evaluation of atherosclerosis.

## 2. MATHEMATICAL MODEL

This present study examines the utilization of permeability in porous media to investigate the dynamics of fluid flow during vascular stenosis in the presence of magnetohydrodynamics (MHD). The utilization of magnetohydrodynamics in physiological issues is garnering increasing interest. We will examine the theoretical framework of incompressible fluid flow within an artery stenosis, where the stenosis has a length denoted by  $L$ . Furthermore, let us assume a cylindrical artery with a stenosis, characterized by a radius denoted as  $\bar{r}$ . It is important to note that the fluid flowing through this artery possesses a certain viscosity  $\bar{\mu}$ . The fluid flow can be organised by smearing enough size of magnetic field. The blood flow axis is denoted as  $\bar{z}$  in this context. The channel is expected to possess a cylindrical configuration, as the blood flow within an artery exhibits characteristics of pipe flow, along direction with velocities  $(\bar{u}, \bar{v}, \bar{w})$  primarily aligned along the  $(\bar{r}, \bar{\theta}, \bar{z})$  axial direction. Here  $\bar{\theta}$  is neglected. Let  $\bar{T}_w$  is the temperature of the outer wall and  $\bar{C}_w$  is the concentration of the outer wall of the artery.

Geometry of the arterial stenosis [30] is symmetric about  $\bar{z}$  direction, which is given by

$$\frac{\bar{R}(z)}{\bar{R}_0(\bar{z})} = \begin{cases} 1 - \frac{\delta_0}{2R_0} \left( 1 + \cos \frac{2\pi}{L_0} \left( \bar{z} - \bar{d} - \frac{L_0}{2} \right) \right) & \text{for } d_0 + L_0 \leq \bar{z} \leq d_0 + 4L_0, \\ 1, & \text{otherwise.} \end{cases} \quad (1)$$



FIGURE 1. Images of a stenosed artery

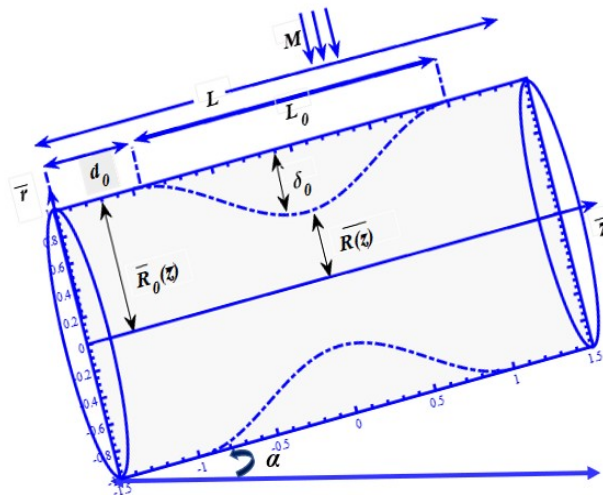


FIGURE 2. Diagram of a stenosed artery

where  $L_0$  is the stenosis length and  $d_0$  the constriction of stenosis.  $\overline{R}(z)$ ,  $\overline{R}_0(\bar{z})$  are the stenosis radius and healthy artery radius respectively.  $n$  decide the compression profile shape and  $\delta_0$  specifies the extreme height of the arterial stenosis situated at

$$\bar{z} = d + \frac{L_0}{n^{\frac{1}{n-1}}}. \quad (2)$$

where  $n = 2$  is extreme height of the stenosis arises at middle-part of the arterial area

$$\bar{z} = d + \frac{L_0}{2}. \quad (3)$$

Since it is considered, the blood is the Newtonian incompressible fluid. The representation in the mathematical model of the artery wall with mild stenosis is given by the authors Kothandapani and Prakash [22], Sharma et al. [23] and Das et al. [30].

Continuity equation

$$\frac{1}{\bar{r}} \frac{\partial(\bar{r}\bar{u})}{\partial\bar{r}} + \frac{\partial\bar{w}}{\partial\bar{z}} = 0 \quad (4)$$

Momentum equation in  $\bar{r}$  direction

$$\rho_{nf}[\bar{u} \frac{\partial\bar{u}}{\partial\bar{r}} + \bar{w} \frac{\partial\bar{u}}{\partial\bar{z}}] = -\frac{\partial\bar{p}}{\partial\bar{r}} + \frac{\partial\bar{\tau}_{\bar{r}\bar{r}}}{\partial\bar{r}} + \frac{\partial\bar{\tau}_{\bar{r}\bar{z}}}{\partial\bar{z}} + g(\rho\beta)_{nf}(\bar{T} - T_0) \cos\alpha \quad (5)$$

Momentum equation in  $\bar{z}$  direction

$$\begin{aligned} \rho_{nf}[\bar{u} \frac{\partial\bar{w}}{\partial\bar{r}} + \bar{w} \frac{\partial\bar{w}}{\partial\bar{z}}] &= -\frac{\partial\bar{p}}{\partial\bar{z}} + \frac{\partial\bar{\tau}_{\bar{r}\bar{z}}}{\partial\bar{r}} + \frac{\partial\bar{\tau}_{\bar{z}\bar{z}}}{\partial\bar{z}} \\ &+ g(\rho\beta)_{nf}(\bar{T} - T_0) \sin\alpha - \frac{\sigma_{nf} B_0^2}{1+m^2}(\bar{w} + m\bar{u}) \end{aligned} \quad (6)$$

Temperature equation

$$(\rho C_p)_{nf}[\bar{u} \frac{\partial\bar{T}}{\partial\bar{r}} + \bar{w} \frac{\partial\bar{T}}{\partial\bar{z}}] = k_{nf}(\frac{\partial^2\bar{T}}{\partial\bar{r}^2} + \frac{1}{\bar{r}} \frac{\partial\bar{T}}{\partial\bar{r}} + \frac{\partial^2\bar{T}}{\partial\bar{z}^2}) - \frac{\partial\bar{q}_r}{\partial\bar{z}} + Q \quad (7)$$

Concentration equation

$$[\bar{u} \frac{\partial\bar{C}}{\partial\bar{r}} + \bar{w} \frac{\partial\bar{C}}{\partial\bar{z}}] = D(\frac{\partial^2\bar{C}}{\partial\bar{r}^2} + \frac{1}{\bar{r}} \frac{\partial\bar{C}}{\partial\bar{r}} + \frac{\partial^2\bar{C}}{\partial\bar{z}^2}) + \frac{DK_T}{T_m}(\frac{\partial^2\bar{T}}{\partial\bar{r}^2} + \frac{1}{\bar{r}} \frac{\partial\bar{T}}{\partial\bar{r}} + \frac{\partial^2\bar{T}}{\partial\bar{z}^2}) \quad (8)$$

where  $\bar{u}$  is the velocity of the blood flow in radial direction,  $B_0^2$  is the applied magnetic field,  $k_{nf}$  is the thermal conductivity of nanofluid,  $\sigma$  is the electrical conductivity,  $\frac{\partial\bar{p}}{\partial\bar{z}}$  is the represents pressure gradient,  $D$  is the mass diffusivity,  $T_m$  is refers to the average temperature of a fluid,  $\rho$  is the density of the fluid,  $C_p$  is the specific heat,  $\frac{\partial\bar{q}_r}{\partial\bar{z}}$  is the radiation effect of heat transfer,  $\bar{q}_r$  represents radiative heat flux in the region.

### Dimensional boundary conditions

$$\frac{\partial\bar{u}}{\partial\bar{r}} = 0, \frac{\partial\bar{T}}{\partial\bar{r}} = 0, \frac{\partial\bar{\sigma}}{\partial\bar{r}} = 0, \text{ at } \bar{r} = 0. \quad (9)$$

$$\bar{u} = 0, \bar{T} = T_0, \bar{\sigma} = 0, \text{ at } \bar{r} = \frac{\bar{R}(\bar{z})}{R(z)}. \quad (10)$$

The axisymmetric arterial vessel necessitates the fulfillment of symmetric boundary conditions for concentration, temperature and velocity over the center line of the channel length.

### Non-dimensional quantity

The equations that govern have been normalized by defining the following non-dimensional parameters, as stated by Sharma et al. [23]. Several non-dimensional factors have been determined and are presented below.

$$\begin{aligned} r &= \frac{\bar{r}}{R_0}, \quad Z = \frac{\bar{Z}}{L_0}, \quad d = \frac{d_0}{L_0}, \quad \delta = \frac{\delta_0}{R_0}, \quad u = \frac{\bar{u}L_0}{\delta U_0}, \\ w &= \frac{\bar{w}}{U_0}, \quad p = \frac{R_0^2 \bar{p}}{U_0 L_0 \mu_f}, \quad \theta = \frac{\bar{T} - T_0}{T_0}, \quad S = \frac{R_0^2 Q}{T_0 k_f}, \quad \sigma = \frac{\bar{C} - C_0}{C_0}. \end{aligned} \quad (11)$$

Williamson fluid referred by Kothandapani and Prakash [22].

$$\bar{\tau}_{\bar{r}\bar{r}} = 2 (1 + We \gamma) \frac{\partial \bar{u}}{\partial \bar{r}} \quad (12)$$

$$\bar{\tau}_{\bar{r}\bar{z}} = (1 + We \gamma) \left( \frac{\partial \bar{u}}{\partial \bar{r}} + \frac{\partial \bar{w}}{\partial \bar{z}} \right) \quad (13)$$

$$\bar{\tau}_{\bar{z}\bar{z}} = 2\mu_0 (1 + We \gamma) \frac{\partial \bar{w}}{\partial \bar{z}} \quad (14)$$

### Non-dimensional governing equation

Applying mild assumption ( $\delta, \frac{R_0}{L_0} < 1$ ) in above equations (4-8).

$$\frac{\partial p}{\partial r} = 0, \quad (15)$$

$$\frac{\partial^2 w}{\partial r^2} \left( 1 + We \frac{\partial w}{\partial r} \right) - \left( \frac{\partial p}{\partial z} - Gr \theta \sin \alpha \right) - \frac{M^2 w}{(1 + m^2)} = 0, \quad (16)$$

$$\frac{\partial^2 \theta}{\partial r^2} (1 + Rn) + \frac{1}{r} \frac{\partial \theta}{\partial r} + S = 0, \quad (17)$$

$$\frac{1}{Sc} \left( \frac{\partial^2 \sigma}{\partial r^2} + \frac{1}{r} \frac{\partial \sigma}{\partial r} \right) - Sr \left( \frac{\partial^2 \theta}{\partial r^2} + \frac{1}{r} \frac{\partial \theta}{\partial r} \right) = 0. \quad (18)$$

### Non-dimensional wall equation and boundary conditions

Applying non dimensional quantity in equation [23] the arterial stenosis is given by

$$R(z) = \begin{cases} 1 - \frac{\delta}{2} (1 + \cos 2\pi (z - d - \frac{1}{2})), & d_0 + 1 \leq \bar{z} \leq d_0 + 4, \\ 1, & \text{otherwise.} \end{cases} \quad (19)$$

$$\frac{\partial u}{\partial r} = 0, \quad \frac{\partial T}{\partial r} = 0, \quad \frac{\partial \sigma}{\partial r} = 0, \quad \text{at } r = 0. \quad (20)$$

$$u = 0, \quad T = 0, \quad \sigma = 0, \quad \text{at } r = R(z). \quad (21)$$

## 3. NUMERICAL SOLVING METHODOLOGY

Equations (16 - 18), which are nonlinear ordinary differential equations, were numerically solved using MATLAB's `bvp4c` function together with equations (20),(21), which specifies the boundary conditions.

In order to facilitate this resolution, the subsequent actions were carried out:

- System Reduction: by adding new variables, the initial set of higher-order partial differential equations was reduced to a set of first-order ordinary differential equations.
- Formulation of Boundary Conditions: In order to guarantee consistency with the restrictions of the problem, boundary conditions were created for the recently included variables.
- Appropriate first approximations for these novel variables were determined, offering a foundation for the numerical solution.
- The intended answer was obtained using the `bvp4c` function by carefully following these procedures, which effectively solved the resultant system.

The governing equations, originally of second-order, were converted into a system of first-order ordinary differential equations with the introduction of new variables. Specifically, the variables  $w$  and  $w'$  were defined as  $y(1)$  and  $y(2)$ , respectively. Additionally, the variables  $\theta$  and  $\theta'$  were defined as  $y(3)$  and  $y(4)$ , while  $\sigma$  and  $\sigma'$  were defined as  $y(5)$  and  $y(6)$ , respectively. The aforementioned process facilitated the conversion of the initial pair of interconnected differential equations of higher order, together with their associated boundary conditions, into a system of five differential equations of first order. Additionally, the boundary conditions were appropriately modified to align with the transformed equations. The system of first-order ordinary differential equations obtained is as follows:

$$w' = y_2, \quad (22)$$

$$w'' = y_2' = \left\{ \frac{1}{(1 + We y(2))} \right\} \left[ \left( \frac{\partial p}{\partial z} - Gr y(3) \sin \alpha \right) + \frac{M^2 y(1)}{(1 + m^2)} \right], \quad (23)$$

$$\theta' = y_4, \quad (24)$$

$$\theta'' = y_4' = - \left\{ \frac{1}{(1 + Rn)} \right\} \left[ \frac{1}{\eta} y(5) + S \right], \quad (25)$$

$$\sigma' = y_6, \quad (26)$$

$$\sigma'' = y_6' = \frac{y(6)}{\eta Sc} - Sr \left\{ \left\{ \frac{1}{(1 + Rn)} \right\} \left[ \frac{1}{\eta} y(5) + S \right] + \frac{y(4)}{\eta} \right\}. \quad (27)$$

The corresponding boundary conditions are

$$y_a(2) = 0, y_b(1) = 0, y_a(4) = 0, \quad (28)$$

$$y_b(3) = 0, y_a(5) = 0, y_b(6) = 0. \quad (29)$$

The employed algorithm is illustrated in figure. 3.

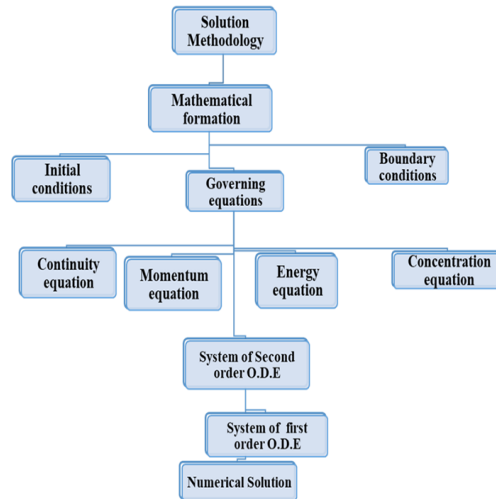


FIGURE 3. Depicts the algorithm employed by the bvp4c procedure in MATLAB.

#### 4. RESULT AND DISCUSSION

In this section, we carried out measurements to assess the influence of various factors on this phenomenon under investigation. These factors include the hall current ( $m$ ), parameter of heat source ( $S$ ), magnetic parameter ( $M$ ), Grashof number ( $Gr$ ), Weissenburg number ( $We$ ), thermal radiation parameter ( $Rn$ ), inclination angle ( $\alpha$ ), Soret number ( $Sr$ ), Schmidt number ( $Sc$ ), as well as profiles of velocity, temperature, and concentration. The following is a list of the physical parameters along with their proposed default values and ranges:  $M$  ranges from 0 to 10,  $m$  ranges from 0 to 1,  $Gr$  ranges from 0 to 10,  $S$  ranges from 0 to 1,  $\phi_1$  ranges from 0 to 0.1,  $\phi_2$  ranges from 0 to 0.1,  $\delta$  ranges from 0.10 to 0.25,  $d$  is fixed at 1,  $z$  is fixed at 1, and  $\alpha$  ranges from 0 to  $\pi/2$ . These values and ranges are based on the studies conducted by Sharma et al. [23] and Das et al. [30]. The effects of these parameters are illustrated in figures 4-15, accompanied by a detailed discussion. The current section is split into three subsections, with the first subsection focusing on the examination of the behavior of axial dimensionless velocity profiles under different parameters. The subsequent subsections provide a demonstration of the impacts of various parameters on the dimensionless temperature and concentration profiles, respectively.

**4.1. Axial Dimensionless Velocity Profile.** The relationship between the velocity of blood and the magnetic field is shown in figure 4, where it is evident that an increase in magnetic field ( $M$ ) values

leads to a decrease in blood velocity. The observed phenomenon can be attributed to the dynamic interplay between the magnetic field and the flow of blood, which gives rise to the emergence of a resistive force commonly referred to as the Lorentz force. The force in question serves as an impediment, hindering the circulation of blood within the constricted artery. An augmentation of  $M$  leads to a decrease in the velocity profile of blood flow in narrowed arteries. Figure 5 depicts how the axial velocity profile changes as the Grashof number ( $Gr$ ) varies. It is evident from the graph that an increase in  $Gr$  causes an increase in the axial velocity profile. This is due to the fact that greater  $Gr$  values generate stronger thermal buoyancy forces, which are predominantly caused by fluctuations in blood density as opposed to hemodynamic forces resulting from blood viscosity. In the blood flow, the prevalence of thermal buoyancy generates vigorous convection currents. Consequently, the blood flow in the artery accelerates significantly as the Grashof number increases. The axial velocity profile is influenced by the Hall parameter ( $m$ ), as depicted in figure 6. Elevated values of the parameter  $m$  result in a corresponding augmentation in the axial velocity. This phenomenon arises due to the positive correlation between the Hall parameter and electron collisions, which subsequently leads to a decrease in the damping magnetic force within the flow. Consequently, there is an increase in blood flow. Moreover, the force resulting from the Hall current acts in opposition to the force generated by the applied magnetic field. Figure 7 illustrates a comparative analysis between a Newtonian fluid ( $We = 0$ ) and a non-Newtonian fluid ( $We > 0$ ) using the Weissenberg number as the basis for comparison. The narrative depicts the correlation between the velocity of a fluid and the Weissenberg number. It is evident that an increase in the Weissenberg number results in a noticeable decrease in the fluid velocity profile. The observed decrease in fluid viscosity can be ascribed to the elevated values of the Weissenberg number, which in turn leads to a lengthened relaxation period for fluid particles. The axial velocity profile changes as the inclination changes, as shown in figure 8. With rising numbers, there is a noticeable improvement in the axial velocity profile. The results also demonstrate that the horizontal artery has the lowest axial velocity ( $\alpha = 0$ ) and the vertical artery has the highest axial velocity ( $\alpha = \pi/2$ ). The relevance of establishing the axial velocity distribution along the artery is highlighted by these observations, which emphasize the impact of inclination angle on fluid flow dynamics.

**4.2. Non-dimensional Temperature Profile.** Figure 9 reveals valuable information regarding the impact of the heat source parameter ( $S$ ) on the temporal changes in temperature within the context of blood flow dynamics. The findings indicate that an increase in  $S$  values is associated with a statistically significant elevation in the distribution of temperature. The central region of the artery exhibits the highest recorded temperature, which progressively diminishes as it approaches the arterial wall. The increase in temperature observed is a direct result of significant heat production occurring within the bloodstream, which can be found in the presence of the heat source. According to figure 10, it

can be observed that augmenting the radiation parameter leads to a corresponding elevation in the temperature profile of the flow. The reason for this phenomenon is that the augmentation of the radiation parameter results in the liberation of thermal energy into the fluid. This observation aligns with the fundamental physics characteristics of the radiation parameter. Figure 11 depicts the effect of solid volume fractions ( $\phi_1, \phi_2$ ) of nanoparticles on temperature distribution. It is clear that increasing the solid volume fractions ( $\phi_1, \phi_2$ ) resulted in a decrease in the blood temperature distribution. This result can be explained by the physical logic that increased nanoparticle concentrations directly alter the thermal diffusivity of the nanofluid, aiding the quick evacuation of heat from the flow regime. As a result, there is a dramatic drop in the temperature distribution within the blood flow.

**4.3. Non-dimensional Concentration Profile.** The parameters of the heat source and the presence of thermal radiation can have a significant impact on the concentration profile. Figure 12 depicts the concentration profile for different thermal radiation values. When thermal radiation values increase, the resulting increase in temperature, greater diffusion, and improved convection typically result in a more homogeneous dispersion of solute throughout the fluid. Consequently, this leads to a reduction in concentration gradients and a drop in the concentration profile. So, the graphic demonstrates a negative correlation between heat radiation ( $Rn$ ) and the concentration of fluid in the stenosis zone of blood flow. Figure 13 illustrates the dimensionless concentration profiles seen at the stenotic neck of the arterial segment, which exhibit a direct relationship with the heat source parameter ( $S$ ). The effects of Schmidt number ( $Sc$ ) on concentration profile are shown in figure 14. An increase in the Schmidt number signifies a considerably higher significance of momentum transport in relation to mass diffusion within the fluid. This phenomenon can give rise to a decelerating process of solute or particle diffusion and mixing, resulting in a concentration profile that is more uniform and exhibits diminished concentration gradients. It is evident from this figure that mass concentration decreases with an increase in the Schmidt number. Figure 15 illustrates the concentration profile for various values of the Soret number. From the figure, it can be observed that as the Soret number ( $Sr$ ) increases, the concentration of fluid in the stenosis region of blood flow also decreases. This phenomenon occurs because of the influence of temperature gradients on species diffusion.

## 5. CONCLUSIONS

The objective of this study is to examine the influence of thermal radiation and hall currents on the flow characteristics of a Williamson nanofluid within an inclined artery that displays mild stenosis. This investigation enhances our understanding of magnetic resonance angiography, a vital radiological diagnostic technique utilized in the evaluation of atherosclerosis. This study investigates the effect of nanoparticles on blood flow difficulties in an inclined channel. The dynamics of the fluid is characterised as laminar and steady. The development of a mathematical model to simulate the impact

of nanoparticles on the hemodynamics of a realistically stenosed scenario. For the inclined channel, ordinary differential equations are derived, and a simplified form of these equations is obtained by incorporating a mild stenotic assumption. The primary outcomes of this study can be summed up as follows:

- (i) Hall current acts in opposition to the force generated by the applied magnetic field.
- (ii) An increase in the Weissenberg number results in a noticeable decrease in the fluid velocity profile.
- (iii) The horizontal artery ( $\alpha = 0$ ) has the lowest axial velocity and the vertical artery ( $\alpha = \pi/2$ ) has the maximum axial velocity.
- (iv) The central region of the artery exhibits the highest recorded temperature, which progressively diminishes as it approaches the arterial wall.
- (v) The solid volume fractions ( $\phi_1, \phi_2$ ) resulted in a decrease in the blood temperature distribution.
- (vi) The dimensionless concentration profiles seen at the stenotic neck of the arterial segment, which exhibits a direct relationship with the heat source parameter ( $S$ ).

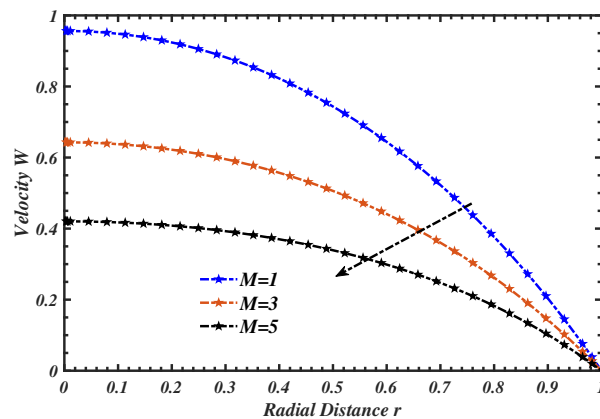


FIGURE 4. Velocity profile Vs Magnetic field( $M$ ) for distinct values of  $M$

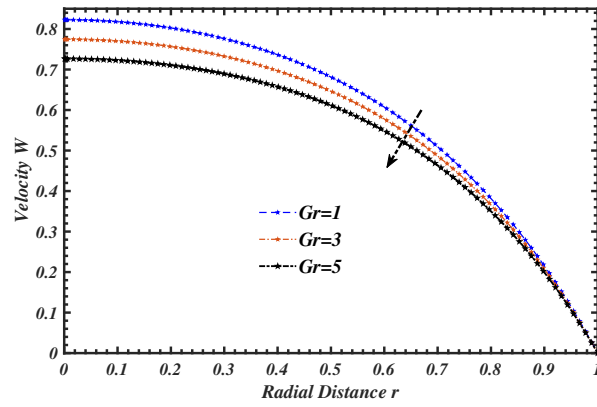


FIGURE 5. Velocity profile Vs Grashof Number ( $Gr$ )

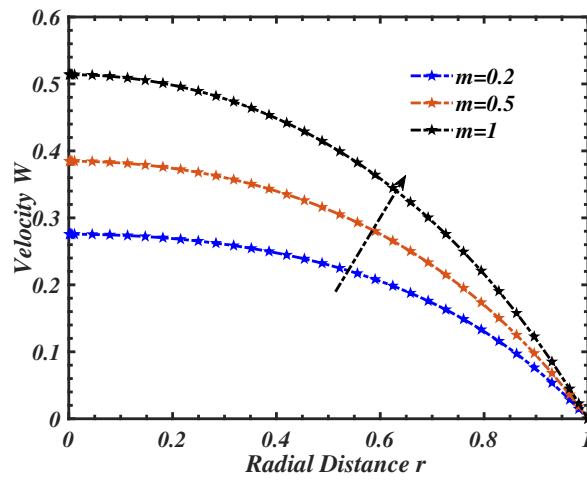


FIGURE 6. Velocity profile Vs Hall Parameter ( $m$ )

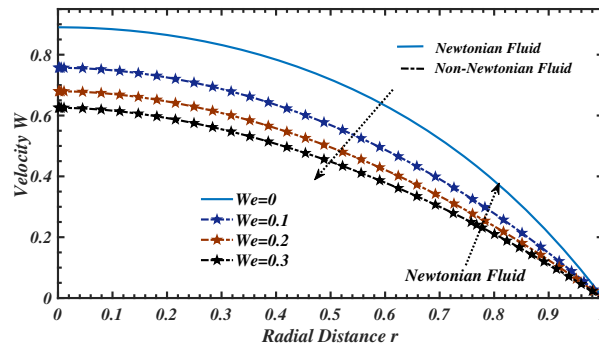


FIGURE 7. Velocity profile Vs Weissenberg Number ( $We$ )

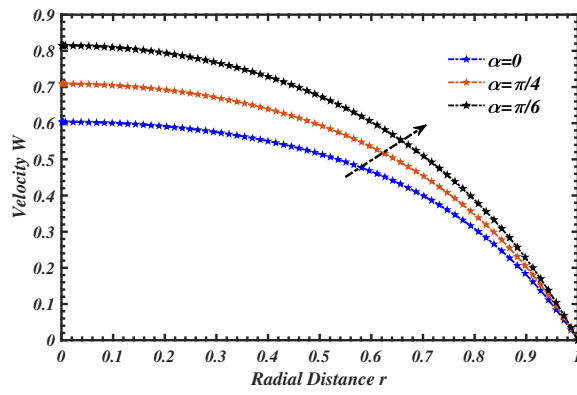


FIGURE 8. Velocity profile Vs Inclined angle ( $\alpha$ )

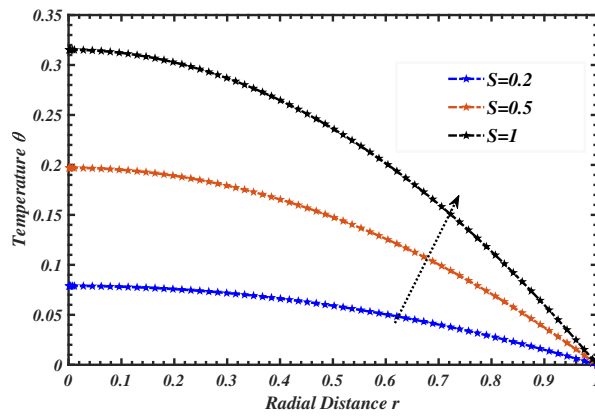


FIGURE 9. Temperature profile Vs Heat Source ( $S$ )

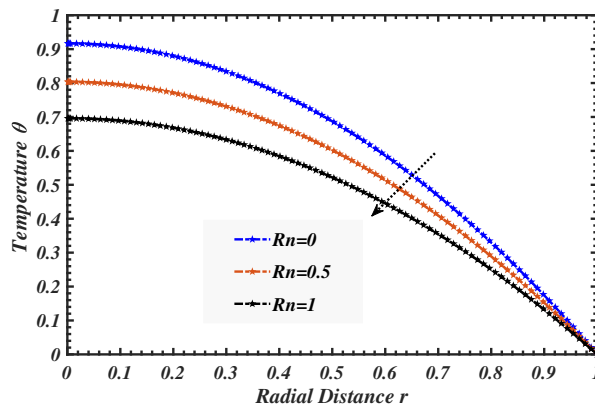
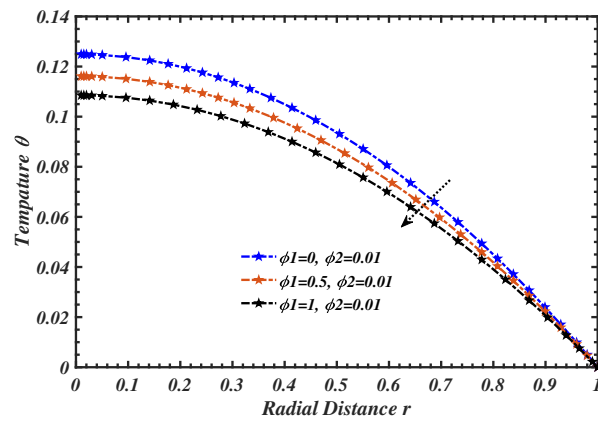
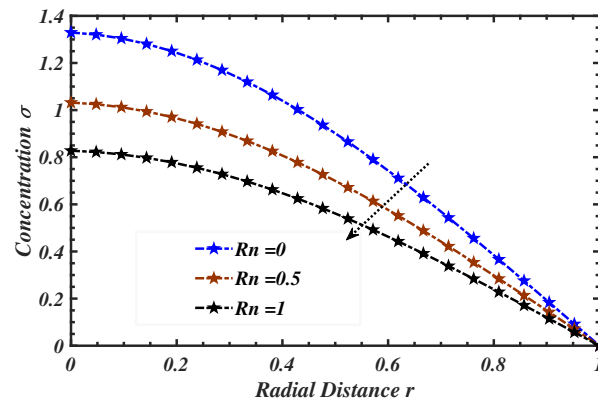
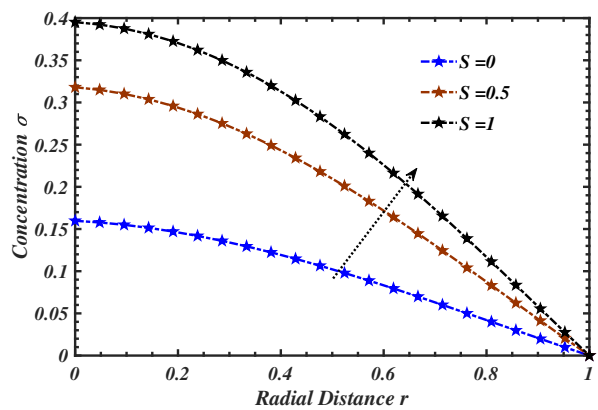
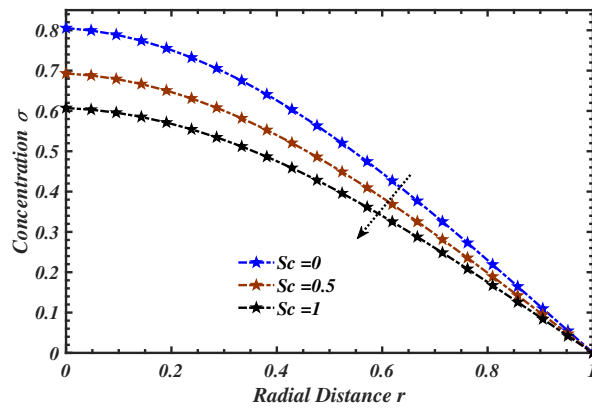
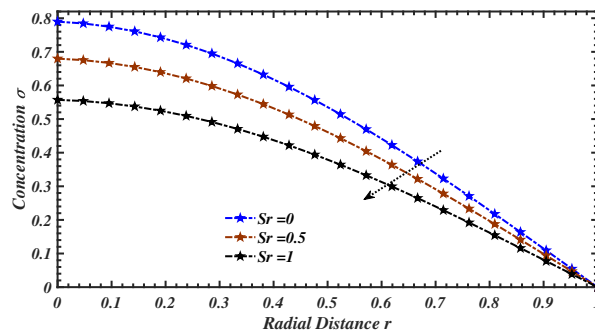


FIGURE 10. Temperature Profile Vs Thermal Radiation( $Rn$ )

FIGURE 11. Temperature Profile Vs varying  $(\phi_1, \phi_2)$ FIGURE 12. Concentration Profile Vs Thermal Radiation( $Rn$ )FIGURE 13. Concentration Profile Vs Heat Source ( $S$ )

FIGURE 14. Concentration Profile Vs Schmidt number ( $Sc$ )FIGURE 15. Concentration Profile Vs Soret Number ( $Sr$ )

## REFERENCES

- [1] H. Jung, J. Choi, C.G. Park, Asymmetric flows of non-Newtonian fluids in symmetric stenosed artery, *Korea Aust. Rheol. J.* 16 (2004), 101–108.
- [2] B. Liu, The influences of stenosis on the downstream flow pattern in curved arteries, *Med. Eng. Phys.* 29 (2007), 868–876. <https://doi.org/10.1016/j.medengphy.2006.09.009>.
- [3] A.K. Qiao, X.L. Guo, S.G. Wu, Y.J. Zeng, X.H. Xu, Numerical study of nonlinear pulsatile flow in S-shaped curved arteries, *Med. Eng. Phys.* 26 (2004), 545–552. <https://doi.org/10.1016/j.medengphy.2004.04.008>.
- [4] A.A. Nejad, Z. Talebi, D. Cheraghali, A. Shahbani-Zahiri, M. Norouzi, Pulsatile flow of non-Newtonian blood fluid inside stenosed arteries: Investigating the effects of viscoelastic and elastic walls, arteriosclerosis, and polycythemia diseases, *Comp. Meth. Programs Biomed.* 154 (2018), 109–122. <https://doi.org/10.1016/j.cmpb.2017.11.016>.
- [5] A. Goswami, S. Ahmed, K.G. Singha, Velocity of Blood flow through uniform rigid artery of human body, *IOSR J. Math.* 13 (2017), 88–92. <https://doi.org/10.9790/5728-1303048892>.
- [6] P. Kalita, R. Schaefer, Mechanical models of artery walls, *Arch. Comp. Meth. Eng.* 15 (2007), 1–36. <https://doi.org/10.1007/s11831-007-9015-5>.
- [7] T. Ishikawa, L.F.R. Guimaraes, S. Oshima, R. Yamane, Effect of non-Newtonian property of blood on flow through a stenosed tube, *Fluid Dyn. Res.* 22 (1998), 251–264. [https://doi.org/10.1016/s0169-5983\(97\)00041-5](https://doi.org/10.1016/s0169-5983(97)00041-5).

- [8] H.T. Basha, R. Sivaraj, Numerical simulation of blood nanofluid flow over three different geometries by means of gyrotactic microorganisms: Applications to the flow in a circulatory system, *Proc. Inst. Mech. Eng. Part C: J. Mech. Eng. Sci.* 235 (2020), 441–460. <https://doi.org/10.1177/0954406220947454>.
- [9] S. Debberma, S. Srivastava, Effect of magnetic field on flow behaviour of blood through a modelled atherosclerotic artery, *Int. Res. J. Eng. Technol.* 8 (2017), 1856–1865.
- [10] K.W. Lee, X.Y. Xu, Modelling of flow and wall behaviour in a mildly stenosed tube, *Med. Eng. Phys.* 24 (2002), 575–586. [https://doi.org/10.1016/s1350-4533\(02\)00048-6](https://doi.org/10.1016/s1350-4533(02)00048-6).
- [11] Q. Long, X.Y. Xu, K.V. Ramnarine, P. Hoskins, Numerical investigation of physiologically realistic pulsatile flow through arterial stenosis, *J. Biomech.* 34 (2001), 1229–1242. [https://doi.org/10.1016/s0021-9290\(01\)00100-2](https://doi.org/10.1016/s0021-9290(01)00100-2).
- [12] S. Sriyab, The Effect of Stenotic Geometry and Non-newtonian Property of Blood Flow through Arterial Stenosis, *Cardiovasc. Hematol. Disord. Drug Targets.* 20 (2020), 16–30. <https://doi.org/10.2174/1871529x19666190509111336>.
- [13] N.S. Sweed, Kh.S. Mekheimer, A. EL-Kholy, A.M. Abdelwahab, Alterations in pulsatile bloodstream with the heat and mass transfer through asymmetric stenosis artery: Erythrocytes suspension model, *Heat Transfer.* 50 (2020), 2259–2287. <https://doi.org/10.1002/htj.21977>.
- [14] A. Zaman, N. Ali, O. Anwar Bég, M. Sajid, Heat and mass transfer to blood flowing through a tapered overlapping stenosed artery, *Int. J. Heat Mass Transfer.* 95 (2016), 1084–1095. <https://doi.org/10.1016/j.ijheatmasstransfer.2015.12.073>.
- [15] S. Das, B. Barman, R.N. Jana, O.D. Makinde, Hall and ion slip currents' impact on electromagnetic blood flow conveying hybrid nanoparticles through an endoscope with peristaltic waves, *BioNanoScience.* 11 (2021), 770–792. <https://doi.org/10.1007/s12668-021-00873-y>.
- [16] Kh.S. Mekheimer, M.A. El Kot, Influence of magnetic field and Hall currents on blood flow through a stenotic artery, *Appl. Math. Mech.-Engl. Ed.* 29 (2008), 1093–1104. <https://doi.org/10.1007/s10483-008-0813-x>.
- [17] N.S. Akbar, A.W. Butt, Magnetic field effects for copper suspended nanofluid venture through a composite stenosed arteries with permeable wall, *J. Magn. Magn. Mater.* 381 (2015), 285–291. <https://doi.org/10.1016/j.jmmm.2014.12.084>.
- [18] M.A. El Kot, Y. Abd Elmaboud, Model of LDL-C concentration of blood flow through a vertical porous microchannel with multiple stenoses: computational simulation, *J. Taibah Univ. Sci.* 17 (2023), 2176194. <https://doi.org/10.1080/16583655.2023.2176194>.
- [19] S. Afzal, M. Qayyum, M.B. Riaz, A. Wojciechowski, Modeling and simulation of blood flow under the influence of radioactive materials having slip with MHD and nonlinear mixed convection, *Alex. Eng. J.* 69 (2023), 9–24. <https://doi.org/10.1016/j.aej.2023.01.013>.
- [20] M.M. Bhatti, M.M. Rashidi, Study of heat and mass transfer with Joule heating on magnetohydrodynamic (MHD) peristaltic blood flow under the influence of Hall effect, *Propuls. Power Res.* 6 (2017), 177–185. <https://doi.org/10.1016/j.jprr.2017.07.006>.
- [21] S.K. Asha, G. Sunitha, Thermal radiation and Hall effects on peristaltic blood flow with double diffusion in the presence of nanoparticles, *Case Stud. Therm. Eng.* 17 (2020), 100560. <https://doi.org/10.1016/j.csite.2019.100560>.
- [22] M. Kothandapani, J. Prakash, Effects of thermal radiation parameter and magnetic field on the peristaltic motion of Williamson nanofluids in a tapered asymmetric channel, *Int. J. Heat Mass Transfer.* 81 (2015), 234–245. <https://doi.org/10.1016/j.ijheatmasstransfer.2014.09.062>.

- [23] B.K. Sharma, C. Kumawat, O.D. Makinde, Hemodynamical analysis of MHD two phase blood flow through a curved permeable artery having variable viscosity with heat and mass transfer, *Biomech. Model. Mechanobiol.* 21 (2022), 797–825. <https://doi.org/10.1007/s10237-022-01561-w>.
- [24] B. Tripathi, B.K. Sharma, Effect of variable viscosity on MHD inclined arterial blood flow with chemical reaction, *Int. J. Appl. Mech. Eng.* 23 (2018), 767–785. <https://doi.org/10.2478/ijame-2018-0042>.
- [25] B. Tripathi, B.K. Sharma, Two-phase analysis of blood flow through a stenosed artery with the effects of chemical reaction and radiation, *Ricerche Mat.* (2021). <https://doi.org/10.1007/s11587-021-00571-7>.
- [26] B.K. Sharma, R. Gandhi, T. Abbas, M.M. Bhatti, Magnetohydrodynamics hemodynamics hybrid nanofluid flow through inclined stenotic artery, *Appl. Math. Mech.-Engl. Ed.* 44 (2023), 459–476. <https://doi.org/10.1007/s10483-023-2961-7>.
- [27] I. Shahzadi, S. Bilal, A significant role of permeability on blood flow for hybrid nanofluid through bifurcated stenosed artery: Drug delivery application, *Comp. Meth. Programs Biomed.* 187 (2020), 105248. <https://doi.org/10.1016/j.cmpb.2019.105248>.
- [28] P. Karmakar, A. Ali, S. Das, Circulation of blood loaded with trihybrid nanoparticles via electro-osmotic pumping in an eccentric endoscopic arterial canal, *Int. Commun. Heat Mass Transfer.* 141 (2023), 106593. <https://doi.org/10.1016/j.icheatmasstransfer.2022.106593>.
- [29] A. Zaman, N. Ali, A.A. Khan, Computational biomedical simulations of hybrid nanoparticles on unsteady blood hemodynamics in a stenotic artery, *Math. Comp. Simul.* 169 (2020), 117–132. <https://doi.org/10.1016/j.matcom.2019.09.010>.
- [30] S. Das, T.K. Pal, R.N. Jana, B. Giri, Significance of Hall currents on hybrid nano-blood flow through an inclined artery having mild stenosis: Homotopy perturbation approach, *Microvasc. Res.* 137 (2021), 104192. <https://doi.org/10.1016/j.mvr.2021.104192>.
- [31] O.U. Mehmood, S. Bibi, D.F. Jamil, S. Uddin, R. Roslan, M.K.M. Akhir, Concentric ballooned catheterization to the fractional non-newtonian hybrid nano blood flow through a stenosed aneurysmal artery with heat transfer, *Sci. Rep.* 11 (2021), 20379. <https://doi.org/10.1038/s41598-021-99499-z>.
- [32] A. Ali, A. Barman, S. Das, EDL aspect in cilia-regulated bloodstream infused with hybridized nanoparticles via a microtube under a strong field of magnetic attraction, *Therm. Sci. Eng. Progress.* 36 (2022), 101510. <https://doi.org/10.1016/j.tsep.2022.101510>.
- [33] T. Elnaqeeb, Modeling of Au(NPs)-blood flow through a catheterized multiple stenosed artery under radial magnetic field, *Eur. Phys. J. Spec. Top.* 228 (2019), 2695–2712. <https://doi.org/10.1140/epjst/e2019-900059-9>.
- [34] M.M. Alanazi, A.A. Hendi, Q. Raza, M.A. Rehman, M.Z.A. Qureshi, B. Ali, N.A. Shah, Numerical computation of hybrid morphologies of nanoparticles on the dynamic of nanofluid: the case of blood-based fluid, *Axioms.* 12 (2023), 163. <https://doi.org/10.3390/axioms12020163>.
- [35] J. Tripathi, B. Vasu, O.A. Bég, R.S.R. Gorla, Unsteady hybrid nanoparticle-mediated magneto-hemodynamics and heat transfer through an overlapped stenotic artery: Biomedical drug delivery simulation, *Proc. Inst. Mech. Eng. Part. H.: J. Eng. Med.* 235 (2021), 1175–1196. <https://doi.org/10.1177/09544119211026095>.
- [36] B. Tripathi, B.K. Sharma, M. Sharma, Modeling and analysis of MHD two-phase blood flow through a stenosed artery having temperature-dependent viscosity, *Eur. Phys. J. Plus.* 134 (2019), 466. <https://doi.org/10.1140/epjp/i2019-12813-9>.

- [37] N.M. Zain, Z. Ismail, Numerical solution of magnetohydrodynamics effects on a generalised power law fluid model of blood flow through a bifurcated artery with an overlapping shaped stenosis, PLoS ONE. 18 (2023), e0276576. <https://doi.org/10.1371/journal.pone.0276576>.
- [38] A. Ahmed, S. Nadeem, Shape effect of Cu-nanoparticles in unsteady flow through curved artery with catheterized stenosis, Results Phys. 7 (2017), 677–689. <https://doi.org/10.1016/j.rinp.2017.01.015>.
- [39] Poonam, B.K. Sharma, C. Kumawat, K. Vafai, Computational biomedical simulations of hybrid nanoparticles (Au-Al<sub>2</sub>O<sub>3</sub>/ blood-mediated) transport in a stenosed and aneurysmal curved artery with heat and mass transfer: Hematocrit dependent viscosity approach, Chem. Phys. Lett. 800 (2022), 139666. <https://doi.org/10.1016/j.cplett.2022.139666>.
- [40] S. Nadeem, N.S. Akbar, T. Hayat, A.A. Hendi, Influence of Heat and Mass Transfer on Newtonian Biomagnetic Fluid of Blood Flow Through a Tapered Porous Arteries with a Stenosis, Transport Porous Media. 91 (2011), 81–100. <https://doi.org/10.1007/s11242-011-9834-6>.
- [41] N. Sher Akbar, S.U. Rahman, R. Ellahi, S. Nadeem, Blood flow study of Williamson fluid through stenosed arteries with permeable walls, Eur. Phys. J. Plus. 129 (2014), 256. <https://doi.org/10.1140/epjp/i2014-14256-2>.